Antiferroelectric topological insulators in ABC compounds

Bartomeu Monserrat,[1,2,*] Joseph W. Bennett,[1] Karin M. Rabe,[1] and David Vanderbilt[1]

[1] *Department of Physics and Astronomy, Rutgers University, Piscataway, New Jersey 08854-8019, USA*
[2] *TCM Group, Cavendish Laboratory, University of Cambridge, J. J. Thomson Avenue, Cambridge CB3 0HE, United Kingdom*

(Dated: February 3, 2017)

We introduce antiferroelectric topological insulators as a new class of functional materials in which an electric field can be used to control topological order and induce topological phase transitions. Using first principles methods, we predict that several orthorhombic members of an ABC family of compounds are antiferroelectric topological insulators. We also show that epitaxial strain and hydrostatic pressure can be used to tune the topological order and the band gap of these ABC compounds. Antiferroelectric topological insulators could enable precise control of topology using electric fields, enhancing the applicability of topological materials in electronics and spintronics.

Topological insulators and related materials [1–3] exhibit unusual properties such as robust edge currents and spin-momentum locking. These unconventional properties have led to a plethora of proposals for the use of topological materials in fundamental research spanning from magnetic monopoles [4] to Majorana fermions [5], and in applications such as fault-tolerant quantum computers. In this context, an innovative route towards the control of topological order is by means of electric fields [6–12].

A promising direction to control topological order with an electric field is to utilize ferroelectric materials that harbor topological states. Ferroelectrics exhibit two states of opposite polarity (**P**) that can be controlled by an electric field (**E**) as shown schematically in Fig. 1a. The two polarization states in these ferroelectric topological insulators could be used, for example, to create spin-selected collimated electron beams [11] or to control the spin texture around the Dirac cones of the surface states [12]. Several materials have been proposed to exhibit these properties: superlattice combinations of the ferroelectric material GeTe and the topological insulator Sb_2Te_3 exhibit electric field control of topological order [8]; strained LiZnSb and $CsPbI_3$ are candidate ferroelectric topological insulators [10, 11]; and ferroelectricity and topological order coexist in some ABC hyperferroelectrics, which could be candidates for thin-film applications [12].

In this work we explore the possibility of controlling topological order in antiferroelectric materials, which exhibit an antipolar ground state and two polar states that can be accessed using an electric field, as shown schematically in Fig. 1b. In ferroelectric materials, the two polar states are related by inversion symmetry, imposing the same topological character on both. Antiferroelectrics are more flexible, as inversion symmetry also dictates that the two polar states have the same topological character, but the antipolar state could belong to a different topological class. We thus define an antiferroelectric topological insulator (AFTI) as an antiferroelectric material in which at least one of the states is a topological insulator. There can be three different types of AFTIs, depending on which states are topological insulators: (i) a type-I AFTI with an antipolar normal state and polar topological states, (ii) a type-II AFTI with an antipolar topological state and polar normal states, and (iii) a type-III AFTI with antipolar and polar topological states. Electric fields could be used to drive topological phase transitions in AFTIs of types I and II. Of these, AFTIs of type I are perhaps the most interesting as their topological polar states would exhibit the properties of ferroelectric topological insulators. The schematic of Fig. 1b shows an example of an AFTI of type I.

We study potential AFTIs in the ABC family of materials which includes compounds that are proposed to be ferroelectric [13], antiferroelectric [14], and hyperferroelectric [15]. The antiferroelectric ABC compounds have a nonpolar reference structure of hexagonal $P6_3/mmc$ space group with energy-lowering distortions to an antipolar orthorhombic $Pnma$ structure and to a polar hexagonal $P6_3mc$ structure. The $Pnma$ antipolar structure is the ground state, and there is a small energy barrier to the $P6_3mc$ polar structure [14]. We adopt a convention in which the B and C atoms form the hexagonal layers of the $P6_3/mmc$ structure, and the A atoms are arranged in the stuffing sites in between. The large

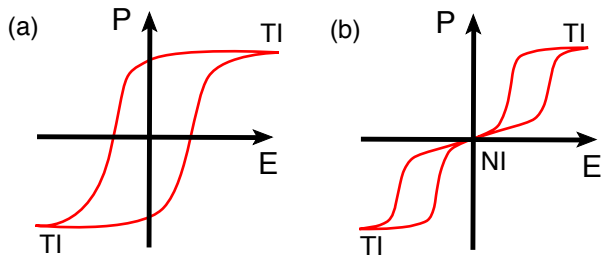

FIG. 1. Schematic representation of (a) a ferroelectric topological insulator and (b) an antiferroelectric topological insulator with an antipolar normal insulator (NI) state and two polar topological insulator (TI) states, referred to as type-I antiferroelectric topological insulator in the text.

number of possible ABC compounds with these characteristics make them an excellent platform to search for the coexistence of antiferroelectricity and other types of order.

Topological insulators exhibit band inversion driven by the spin-orbit interaction. Since the strength of the spin-orbit interaction increases with the atomic number, we focus the search for topological materials in ABC compounds to those containing heavy elements. Furthermore, the energy scale associated with spin-orbit coupling (of up to about 1 eV) needs to be comparable to the band gap in order to induce a band inversion, and therefore we focus on materials with band gaps below 1 eV. We use these criteria to search over the ABC antiferroelectrics reported in Ref. [14], and we indentify three compounds, LiMgBi, NaMgBi, and KMgBi, that are promising candidates as AFTIs. We refer collectively to these three compounds as AMgBi (for A =Li, Na, K).

First-principles calculations. Our calculations are based on density functional theory (DFT) as implemented in the VASP package [16–19]. We use the local density approximation to the exchange correlation functional [20, 21] and the projector augmented wave method [22, 23] with an energy cut-off of 300 eV and a $\mathbf{k}$-point grid size of $8\times8\times8$ to sample the Brillouin zone (BZ). All calculations include spin-orbit coupling. The lattice vectors and internal coordinates are optimized until the forces on all atoms are smaller than 0.001 eV/Å, and the pressure is within 0.01 GPa of the target value when applying hydrostatic pressure. In-plane epitaxial strain on a hexagonal lattice is imposed by constraining the in-plane lattice constants and allowing the out-of-plane lattice constant and the internal coordinates to fully relax. Strains are reported using the hexagonal $P6_3mc$ equilibrium structure as reference, with in-plane lattice constants equal to 4.68 Å, 4.86 Å, and 5.05 Å for LiMgBi, NaMgBi, and KMgBi, respectively. The $Pnma$ equilibrium structure differs from any epitaxially strained $Pnma$ structure because the imposition of a hexagonal substrate forces the two in-plane lattice vectors of the orthorhombic structure to have the exact ratio $\sqrt{3}$, a condition that is not exactly obeyed in the unstrained structure.

We make a precise determination of the band gaps by Wannier interpolation of the band structure [24] using the WANNIER90 package [25, 26]. We use the iterative approach of Ref. [27], initially sampling the electronic BZ with a coarse $\mathbf{k}$ grid (typically of size $40\times40\times40$), then determining the $\mathbf{k}_0$-point having the smallest gap, and then searching over a denser $\mathbf{k}$-point grid centered around the point $\mathbf{k}_0$. This procedure is iterated until convergence is reached. Once we have determined that a phase is insulating, we calculate the topological Z_2 index by following the adiabatic pumping of Wannier charge centers over the BZ [28] as implemented in the Z2PACK code [29]. This approach is appropriate for systems without inversion symmetry.

TABLE I. Energy difference ΔE between the $P6_3mc$ structure and the $Pnma$ structure in meV per formula unit (f.u.), and the band gaps $E_g^{P6_3mc}$ and E_g^{Pnma} of the $P6_3mc$ and the $Pnma$ structures in meV. All results correspond to the equilibrium structures.

	ΔE (meV/f.u.)	$E_g^{P6_3mc}$ (meV)	E_g^{Pnma} (meV)
LiMgBi	59	66	12
NaMgBi	122	85	22
KMgBi	239	96	16

Equilibrium structures. The $Pnma$ structure is lower in energy compared to the $P6_3mc$ structure in all three AMgBi materials, as shown in Table I. All three materials in both the $P6_3mc$ and $Pnma$ structures are strong topological insulators with topological indices (1; 000). The minimum band gaps, shown in Table I, occur near the Γ point, with states dominated by bismuth and magnesium. These results indicate that the AMgBi compounds are candidate topological insulators. Furthermore, as they are also candidate antiferroelectrics, these materials become candidate AFTIs of type III in which the the antipolar and both polar states have the same Z_2 indices.

Epitaxial strain. The equilibrium structures are type III candidate AFTIs, but it would be desirable to find AFTIs of types I and II as well. With this aim, we fur-

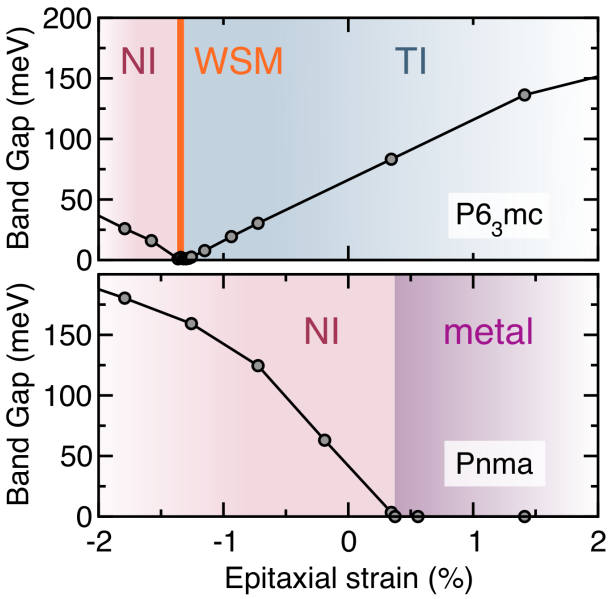

FIG. 2. Band gap of the LiMgBi compound of polar $P6_3mc$ (top) and antipolar $Pnma$ (bottom) structures as a function of epitaxial strain. The $P6_3mc$ struture exhibits regions in which it is a topological insulator (TI), a Weyl semimetal (WSM), and a normal insulator (NI), whereas the $Pnma$ structure exhibits metallic and normal insulator phases.

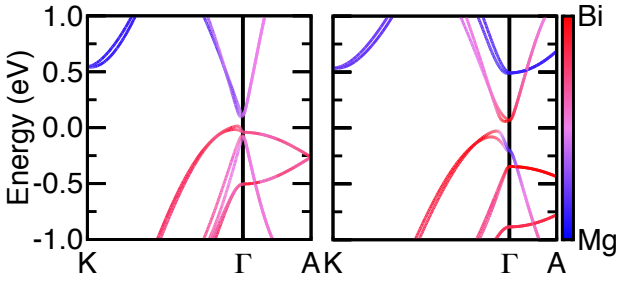

FIG. 3. Band structure of LiMgBi in the polar $P6_3mc$ structure at strains of -2.9% (left) corresponding to a normal insulator, and $+0.3\%$ (right) corresponding to a topological insulator.

ther investigate how the relative energies between the $Pnma$ and $P6_3mc$ structures, as well as their topological character, can be tuned by means of epitaxial strain. We find that the unstrained $P6_3mc$ structure of all three compounds corresponds to a topological insulator, and compressive epitaxial strain drives them through a topological phase transition to a normal insulator via an intermediate Weyl semimetal phase, as shown in Fig. 2 for LiMgBi. The intermediate semimetallic phase is a universal feature of a topological phase transition in materials without inversion symmetry [27, 30]. In Fig. 3 we show the band structure of polar $P6_3mc$ LiMgBi around the Γ point for epitaxial strains of -2.86%, corresponding to a normal insulator, and $+0.34\%$, corresponding to a topological insulator, with gaps of 93 and 94 meV respectively. The bands exhibit Rashba splitting, the strength of which can also be tuned by means of epitaxial strain. The projection on the bismuth orbitals demonstrates the band inversion associated with the topological phase transition.

In LiMgBi, the epitaxially strained $Pnma$ structure is a normal insulator under compressive strain, and becomes a metal at about 0.34% tensile strain (Fig. 2). The fact that the epitaxial LiMgBi $Pnma$ structure is either a normal insulator or a metal, whereas the corresponding unstrained structure is a topological insulator, derives from the fixed $\sqrt{3}$ ratio that the two in-plane orthorhombic axes obey under epitaxial strain. The violation of this condition is largest in LiMgBi, reaching 8%, whereas it is 6% in NaMgBi, and almost perfectly obeyed in KMgBi. We have performed band gap and Z_2 index calculations of several LiMgBi structures linearly interpolating between the epitaxially strained and unstrained $Pnma$ structures, confirming that there is a gap closure and a topological phase transition from the unstrained topological insulator to the epitaxial normal insulator.

The band gap results presented in Fig. 2 indicate that epitaxial LiMgBi is a candidate AFTI of type I with the polar states corresponding to a topological insulator, and the antipolar state to a normal insulator, the situation depicted in Fig 1b. Moreover, the energy difference between the $Pnma$ and the $P6_3mc$ structures decreases from 59 meV for the equilibrium configuration (see Table I) to 18 meV at zero strain, and the difference decreases further with increasing compressive strain, promoting the possibility that an electric field can be used to switch between the polar and antipolar states. Finally, we note that a polymorph of LiMgBi, namely MgLiBi in which the Li and Mg atoms are exchanged, is more stable for compressive strains above 0.20%, so that the potential synthesis of LiMgBi as an AFTI should focus in the epitaxial strain range from -0.20% to $+0.34\%$.

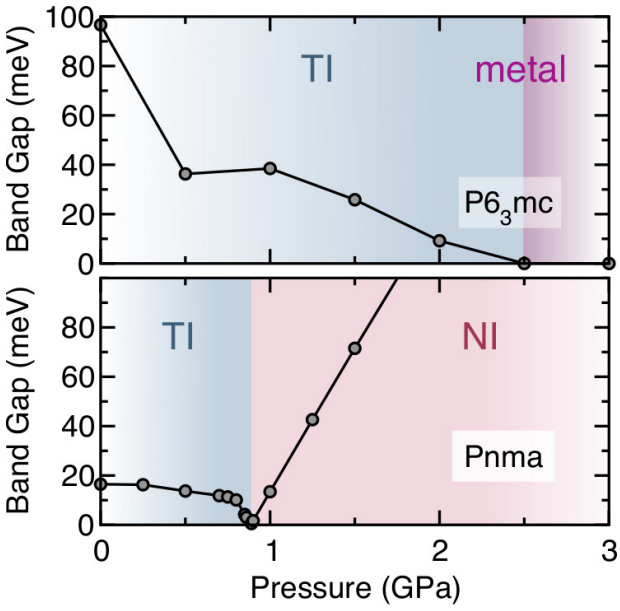

FIG. 4. Band gap of the KMgBi compound of polar $P6_3mc$ (top) and antipolar $Pnma$ (bottom) structures as a function of hydrostatic pressure. The $P6_3mc$ struture exhibits a topological insulator (TI) regime and a metallic regime, whereas the $Pnma$ structure exhibits topological insulator and normal insulator (NI) phases.

In NaMgBi and KMgBi, the $Pnma$ structure under epitaxial strain does not exhibit a normal insulator regime, and therefore an antipolar normal state cannot coexist with a polar topological state in these materials. Instead, in NaMgBi a polar normal insulator coexists with an antipolar topological insulator at strains between -4.72% and -4.00%, which corresponds to a type-II AFTI. However, the band gap for both antipolar and polar states in that region is below 20 meV, which may make experimental realization difficult. KMgBi under strain behaves analogously to NaMgBi, and the polar normal insulator coexists with the antipolar topological insulator at strains between -4.95% and -3.96%, but again the band gaps are small. Additional details of NaMgBi and KMgBi under strain are provided in the Supplemental Material.

Hydrostatic pressure. Under hydrostatic pressure, the $P6_3mc$ structure of NaMgBi and KMgBi undergoes a

TABLE II. Candidate AFTIs from the AMgBi family of compounds. Type I refers to normal antipolar and topological polar states, type II to topological antipolar and normal polar states, and type III to topological antipolar and polar states.

	Equilibrium	Epitaxial strain	Pressure
LiMgBi	–	Type I (−0.20% to +0.34%)	–
NaMgBi	Type III	Type II (−4.72% to −4.00%)	–
KMgBi	Type III	Type II (−4.95% to −3.96%)	Type I (0.89 GPa to 2.50 GPa)

transition from a topological insulator into a metal, as shown in Fig. 4 for KMgBi. The *Pnma* structure of NaMgBi and KMgBi undergoes a topological phase transition from a topological to a normal insulator, as shown for KMgBi in Fig. 4. LiMgBi under hydrostatic pressure is higher in energy than the polymorph MgLiBi.

The band gap results of Fig. 4 suggest that KMgBi under hydrostatic pressure is also a candidate AFTI of type I (Fig. 1b). In particular, this functional phase should be observable at pressure between 0.89 GPa and 2.50 GPa. NaMgBi has a phase diagram similar to that of KMgBi, but there is no pressure range in which the normal antipolar and topological polar phases coexist, as shown in the Supplemental Material.

Discussion. Overall, our first-principles calculations indicate that the AMgBi compounds are promising candidates as AFTIs, as summarized in Table II. Of these, the most promising candidates are LiMgBi under epitaxial strain in the range from −0.20% to +0.34%, and KMgBi under hydrostatic pressure between 0.89 GPa and 2.50 GPa, which are AFTIs of type I with polar topological states and an antipolar normal state as depicted in Fig. 1b. In these materials, an electric field could be used to induce a topological phase transition. This possibility raises interesting questions for future research, such as the precise switching mechanism in AFTIs (as well as in ferroelectric topological insulators). Switching typically occurs via the motion of domain walls, but in an AFTI of type I or II these domain walls separate phases of distinct topological order. As a result they are necessarily metallic, which may influence the switching dynamics in unusual and interesting ways.

Conclusions. We propose a new type of functional material, an antiferroelectric topological insulator, in which an electric field can be used to induce topological phase transitions and to control topological order. Using first-principles methods, we show that the orthorhombic ABC compounds provide a rich playground in which to explore the existence of antiferroelectric topological insulators. In particular, the compounds AMgBi (A =Li, Na, K) exhibits an interesting interplay between antiferroelectric and topological properties as a function of both epitaxial strain and hydrostatic pressure, with LiMgBi under strain and KMgBi under pressure appearing as promising candidates for the experimental realization of an antiferroelectric topological insulator.

This work was funded by NSF grant DMR-1408838 and the Office of Naval Research grant N00014-12-1-1040. B.M. thanks Robinson College, Cambridge, and the Cambridge Philosophical Society for a Henslow Research Fellowship.

* monserrat@physics.rutgers.edu

[1] C. L. Kane and E. J. Mele, "Z_2 topological order and the quantum spin Hall effect," Phys. Rev. Lett. **95**, 146802 (2005).
[2] M. Z. Hasan and C. L. Kane, "*Colloquium*: Topological insulators," Rev. Mod. Phys. **82**, 3045–3067 (2010).
[3] Xiao-Liang Qi and Shou-Cheng Zhang, "Topological insulators and superconductors," Rev. Mod. Phys. **83**, 1057–1110 (2011).
[4] Xiao-Liang Qi, Rundong Li, Jiadong Zang, and Shou-Cheng Zhang, "Inducing a magnetic monopole with topological surface states," Science **323**, 1184–1187 (2009).
[5] Liang Fu and C. L. Kane, "Superconducting proximity effect and Majorana fermions at the surface of a topological insulator," Phys. Rev. Lett. **100**, 096407 (2008).
[6] Minsung Kim, Choong H. Kim, Heung-Sik Kim, and Jisoon Ihm, "Topological quantum phase transitions driven by external electric fields in Sb_2Te_3 thin films," Proc. Natl. Acad. Sci. U.S.A. **109**, 671–674 (2012).
[7] Tong Zhang, Jeonghoon Ha, Niv Levy, Young Kuk, and Joseph Stroscio, "Electric-field tuning of the surface band structure of topological insulator Sb_2Te_3 thin films," Phys. Rev. Lett. **111**, 056803 (2013).
[8] J. Tominaga, A. V. Kolobov, P. Fons, T. Nakano, and S. Murakami, "Ferroelectric order control of the Dirac-semimetal phase in GeTe-Sb_2Te_3 superlattices," Adv. Mater. Interfaces **1**, 1300027 (2014).
[9] Qihang Liu, Xiuwen Zhang, L. B. Abdalla, Adalberto Fazzio, and Alex Zunger, "Switching a normal insulator into a topological insulator via electric field with application to phosphorene," Nano Lett. **15**, 1222 (2015).
[10] Awadhesh Narayan, "Class of Rashba ferroelectrics in hexagonal semiconductors," Phys. Rev. B **92**, 220101 (2015).
[11] Shi Liu, Youngkuk Kim, Liang Z. Tan, and Andrew M. Rappe, "Strain-induced ferroelectric topological insulator," Nano Lett. **16**, 1663 (2016).
[12] Domenico Di Sante, Paolo Barone, Alessandro Stroppa, Kevin F. Garrity, David Vanderbilt, and Silvia Picozzi, "Intertwined Rashba, Dirac, and Weyl fermions in hexagonal hyperferroelectrics," Phys. Rev. Lett. **117**, 076401 (2016).
[13] Joseph W. Bennett, Kevin F. Garrity, Karin M. Rabe,

and David Vanderbilt, "Hexagonal *ABC* semiconductors as ferroelectrics," Phys. Rev. Lett. **109**, 167602 (2012).
[14] Joseph W. Bennett, Kevin F. Garrity, Karin M. Rabe, and David Vanderbilt, "Orthorhombic *ABC* semiconductors as antiferroelectrics," Phys. Rev. Lett. **110**, 017603 (2013).
[15] Kevin F. Garrity, Karin M. Rabe, and David Vanderbilt, "Hyperferroelectrics: Proper ferroelectrics with persistent polarization," Phys. Rev. Lett. **112**, 127601 (2014).
[16] G. Kresse and J. Hafner, "*Ab initio* molecular dynamics for liquid metals," Phys. Rev. B **47**, 558 (1993).
[17] G. Kresse and J. Hafner, "*Ab initio* molecular-dynamics simulation of the liquid-metal-amorphous-semiconductor transition in germanium," Phys. Rev. B **49**, 14251 (1994).
[18] G. Kresse and J. Furthmüller, "Efficiency of ab-initio total energy calculations for metals and semiconductors using a plane-wave basis set," Comput. Mater. Sci. **6**, 15 (1996).
[19] G. Kresse and J. Furthmüller, "Efficient iterative schemes for *ab initio* total-energy calculations using a plane-wave basis set," Phys. Rev. B **54**, 11169 (1996).
[20] D. M. Ceperley and B. J. Alder, "Ground state of the electron gas by a stochastic method," Phys. Rev. Lett. **45**, 566–569 (1980).
[21] J. P. Perdew and Alex Zunger, "Self-interaction correction to density-functional approximations for many-electron systems," Phys. Rev. B **23**, 5048–5079 (1981).
[22] P. E. Blöchl, "Projector augmented-wave method," Phys. Rev. B **50**, 17953 (1994).
[23] G. Kresse and D. Joubert, "From ultrasoft pseudopotentials to the projector augmented-wave method," Phys. Rev. B **59**, 1758 (1999).
[24] Nicola Marzari, Arash A. Mostofi, Jonathan R. Yates, Ivo Souza, and David Vanderbilt, "Maximally localized Wannier functions: Theory and applications," Rev. Mod. Phys. **84**, 1419–1475 (2012).
[25] Arash A. Mostofi, Jonathan R. Yates, Young-Su Lee, Ivo Souza, David Vanderbilt, and Nicola Marzari, "wannier90: A tool for obtaining maximally-localised Wannier functions," Comput. Phys. Commun. **178**, 685 – 699 (2008).
[26] Arash A. Mostofi, Jonathan R. Yates, Giovanni Pizzi, Young-Su Lee, Ivo Souza, David Vanderbilt, and Nicola Marzari, "An updated version of wannier90: A tool for obtaining maximally-localised Wannier functions," Comput. Phys. Commun. **185**, 2309 – 2310 (2014).
[27] Jianpeng Liu and David Vanderbilt, "Weyl semimetals from noncentrosymmetric topological insulators," Phys. Rev. B **90**, 155316 (2014).
[28] Alexey A. Soluyanov and David Vanderbilt, "Computing topological invariants without inversion symmetry," Phys. Rev. B **83**, 235401 (2011).
[29] Dominik Gresch, Gabriel Autès, Oleg V. Yazyev, Matthias Troyer, David Vanderbilt, B. Andrei Bernevig, and Alexey A. Soluyanov, "Z2Pack: Numerical implementation of hybrid Wannier centers for identifying topological materials," arXiv:1610.08983 (2016).
[30] Shuichi Murakami and Shun-ichi Kuga, "Universal phase diagrams for the quantum spin Hall systems," Phys. Rev. B **78**, 165313 (2008).